Identification and quantification of gold engineered nanomaterials and impaired fluid transfer across the rat placenta via ex vivo perfusion

Biomedicine & Pharmacotherapy 117 (2019) 109148

Contents lists available at ScienceDirect

Biomedicine & Pharmacotherapy

journal homepage: www.elsevier.com/locate/biopha

Identification and quantification of gold engineered nanomaterials and impaired fluid transfer across the rat placenta *via ex vivo* perfusion

J.N. D'Errico[a], C. Doherty[b], S.B. Fournier[b], N. Renkel[b], S. Kallontzi[c], M. Goedken[d], L. Fabris[c], B. Buckley[b], P.A. Stapleton[a,b,*]

[a] Department of Pharmacology and Toxicology, Ernest Mario School of Pharmacy, Rutgers University, 160 Frelinghuysen Rd., Piscataway, NJ 08854, USA
[b] Environmental and Occupational Health Sciences Institute, 170 Frelinghuysen Rd., Piscataway, NJ 08854, USA
[c] Department of Material Science and Engineering, School of Engineering, Rutgers University, 607 Taylor Rd., Piscataway, NJ 08854, USA
[d] Research Pathology Services, Rutgers University, Piscataway, NJ 08854, USA

ARTICLE INFO

Keywords:
Placenta
Engineered nanomaterial
Organ perfusion
Gold nanomaterials
ICP-MS

ABSTRACT

Development and implementation of products incorporating nanoparticles are occurring at a rapid pace. These particles are widely utilized in domestic, occupational, and biomedical applications. Currently, it is unclear if pregnant women will be able to take advantage of the potential biomedical nanoproducts out of concerns associated with placental transfer and fetal interactions. We recently developed an *ex vivo* rat placental perfusion technique to allow for the evaluation of xenobiotic transfer and placental physiological perturbations. In this study, a segment of the uterine horn and associated placenta was isolated from pregnant (gestational day 20) Sprague-Dawley rats and placed into a modified pressure myography vessel chamber. The proximal and distal ends of the maternal uterine artery and the vessels of the umbilical cord were cannulated, secured, and perfused with physiological salt solution (PSS). The proximal uterine artery and umbilical artery were pressurized at 80 mmHg and 50 mmHg, respectively, to allow countercurrent flow through the placenta. After equilibration, a single 900 µL bolus dose of 20 nm gold engineered nanoparticles (Au-ENM) was introduced into the proximal maternal artery. Distal uterine and umbilical vein effluents were collected every 10 min for 180 min to measure placental fluid dynamics. The quantification of Au-ENM transfer was conducted *via* inductively coupled plasma mass spectrometry (ICP-MS). Overall, we were able to measure Au-ENM within uterine and umbilical effluent with 20 min of material infusion. This novel methodology may be widely incorporated into studies of pharmacology, toxicology, and placental physiology.

1. Introduction

Treatment of a woman during pregnancy is a delicate balance between maternal therapy and fetal risk. Maternal exposure to xenobiotic pharmaceuticals, particles, or chemicals during gestation can lead to spontaneous abortion, fetal malformations, and developmental onset of disease [1,2]. Central to this unique environment is the placenta, a temporary organ that functions as a barrier to prevent passage of unwanted xenobiotics and that transfers nutrients in exchange for waste. Therefore, it is critical to understand the passage of pharmaceuticals and xenobiotic particles from the maternal to the fetal compartment.

Development and implementation of products incorporating nanoparticles are occurring at a rapid pace. These pervasive particles are widely utilized, with many domestic, occupational, and biomedical applications. Gold nanoparticles (Au-ENM) have demonstrated a great potential in biosensing, imaging, and theranostic applications [3–5]. Gold nanoparticles are given as an intravenous injection in the clinic for the purpose of contrast imaging for diagnostic procedures [6,7]. These applications can be expanded by modifying the physicochemical properties of the material (*e.g.*, material, size, shape, inclusion of functionalized groups) making them more useful, but in turn altering the biological interactions, pharmacological function, and toxicological relevance [4,8,9]. Increasing biomedical applications and consumer use products have led to domestic unintentional exposures, including during pregnancy [8,10–12]. Therefore, understanding ENM behavior and prenatal and perinatal outcomes of ENM exposure is paramount.

Few studies have comprehensively evaluated ENM translocation from the maternal blood and deposition within the placenta and fetus

* Corresponding author at: Department of Pharmacology and Toxicology, Ernest Mario School of Pharmacy, Environmental and Occupational Health Sciences Institute, Rutgers University, 170 Frelinghuysen Road, Piscataway, NJ 08854, USA.
E-mail address: stapleton@eohsi.rutgers.edu (P.A. Stapleton).

https://doi.org/10.1016/j.biopha.2019.109148
Received 1 May 2019; Received in revised form 14 June 2019; Accepted 17 June 2019

after intravenous injection during pregnancy [13–18]. Using ENM with a wide variety of physiochemical properties, previous studies have demonstrated translocation to the embryo of gold [17], silica [18], titanium-dioxide [18], functionalized-mesoporous silica [13], and functionalized carbon in the forms of pegylated (PEG) single-walled carbon nanotubes [15] and radiolabeled fullerenes [16]. However, it is unclear from these studies how quickly ENM passage occurs from the maternal circulation to the fetal compartment and if this transport acutely impairs normal placental function with respect to blood flow and nutrient delivery.

Experiments using *ex vivo* human placental perfusion of a single cotyledon to investigate passage of functionalized Au-ENM (3–4 nm) to the fetal compartment after 6 h of infusion identified passage of PEG-Au-ENM but no passage of carboxylated-Au-ENM [19]. Interestingly, recirculating human placental perfusion studies of 10, 15, and 30 nm PEG-Au-ENM demonstrates no transfer to fetal effluent [20]. Similar experiments to evaluate size-dependent passage of fluorescent polystyrene ENM have been conducted [21]. These *ex vivo* studies identified passage of ENM 50–300 nm in diameter across the placenta in both maternal-to-fetal and fetal-to-maternal directions without compromising cellular survival [21,22]. ENM modifications, including non-uniformity of particle size and/or surface modifications designed to increase material biomedical functionality or prevent particle agglomeration will alter the kinetics of ENM transfer across the human placenta [23]. Investigations using human tissue are exceedingly valuable, but have limitations. These studies are technically demanding, require specialized equipment, and are limited by tissue access. Investigations of disease or pre-term xenobiotic transfer using human tissue may not be possible given ethical considerations. Investigators [11,24,25] have called for the need of additional studies focused of placental transfer of ENM and for confirmation of the physiochemical properties of ENM used within toxicological studies.

The mouse is the most commonly used animal model to study the placenta, and *ex vivo* mouse placental perfusion techniques have been established [26,27]. Use of this species as a model is beneficial for physiological and mechanistic studies due to genetic manipulation capabilities. While the mouse model exhibits the same hemochorial placentation classification and analogous cell types, there are distinct differences to humans. Mouse placentas do not have trophoblastic cells that invade the myometrium or spiral arterioles of the maternal uterus [28]. Rat placentas show more similarities to humans at the site of maternal-fetal interface and do reflect the deep uterine vascular invasion and remodeling [29]. Therefore, *ex vivo* rat placental perfusion is advantageous for toxicological and pharmacological investigations, as the test article maternal-fetal kinetics can be more relevant for extrapolation to humans.

We recently developed a novel *in situ* rat placental perfusion methodology for toxicological studies [30]. Without morphological or physiological impairment, this methodology permits the measurement of fluid transport across the placenta in addition to maternal/fetal kinetics of the xenobiotic. Previous descriptions of isolated rat placenta have reported solute transfer solely from the fetus to the maternal blood [31,32]. Use of the dually-perfused isolated rat placenta has led to the assessments of phosphate, calcium, and chloride solute transport across the placenta [33–35], cyclosporine transfer [36], barrier activity [37], and in some cases, to reporting physiological adaptations of the placenta to environmental changes (*e.g.* hypoxia) [38]. However, none of these studies have been completed with a pharmacological or toxicological focus to assess the passage of xenobiotic particles from the maternal circulation to the developing fetus [26]. Therefore, the purpose of this study was to identify the transfer of Au-ENM from the maternal to fetal compartment, record the time course of this transfer, and assess the placental physiological reactivity after Au-ENM infusion. While previous work has demonstrated nanoparticle translocation to the fetal compartment after 24 h, we hypothesize that transfer from the maternal circulation, across the placental barrier, and into the fetal compartment occurs within minutes. We further hypothesize that this transfer will impair placental hemodynamics and reduce blood flow to the developing fetus.

2. Methods

2.1. Animals

Sprague Dawley rats were purchased time-pregnant from Charles River Laboratories (Kingston, NY). Animals were delivered at least 48-h before use and acclimated within the AAALAC accredited facilities at Rutgers University with food and water available *ad libitum*. Animal sacrifice and placental perfusions took place at full term on GD 20. All procedures were approved by the Institutional Animal Care and Use Committee of Rutgers University.

2.2. ENM characterization

Stock solution of 20 nm naïve gold nanoparticle spheres (gold ENM; 7×10^{11} particles/mL; GP01-20-100; NanoCS, New York, NY) was suspended in 0.01% sodium citrate and sonicated for 15 min prior to measurement. The average agglomerate size was identified as 49.89 nm ± 0.16 *via* dynamic light scattering (DLS) techniques using Zetasizer Nano ZS by Malvern. The size of the nanoparticles was measured with Non-Invasive Backscatter optics (NIBS) using a 4 mW, 633 nm laser. The ENM ζ-potential was also measured *via* Zetasizer Nano ZS.

2.3. Placental isolation

Under isoflurane general anesthesia (5% induction and 2% maintenance), the central placental unit of the right uterine horn was isolated, excised and transferred into cold physiological salt solution (PSS). Briefly, the uterine vasculature was ligated, and the placental unit with uterine muscle, placenta, amniotic sac, fetal pup, umbilical cord, and the supporting vasculature removed. Prior to extracting the fetus, uterine muscle was retracted, amniotic membranes removed, umbilical cord unraveled, umbilical vasculature identified and separated, as previously published [30].

2.4. Placental perfusion

The placental unit was placed within a modified isolated vessel chamber (Living Systems Instrumentation, Burlington, VT) (Fig. 1) filled with warmed, oxygenated, circulating PSS. The proximal and distal ends of the uterine artery were cannulated with glass pipettes measuring 75–100 μm at the tips and secured using 11-0 nylon suture (Alcon). The umbilical artery and vein were cannulated using 4-inch 26 g blunt needles and secured with 11-0 nylon suture. The uterine artery was perfused *via* a peristaltic pump with PSS at 80 mmHg and perfusate was collected from the distal end. The umbilical artery was perfused with gravity-fed PSS at 50 mmHg and fetal effluent was collected from the umbilical vein cannula. Steps for this procedure can be accessed in further detail in our previous technical publication [30]. After cannulation and 20-min equilibration, baseline perfusion effluent was collected for 10 min prior to ENM infusion and sample collection continued to occur in 10-min intervals for a total of 180 min. Further, fluid that remained in the 4" pipette cannulating the umbilical vein was also collected and identified as residual effluent (R).

2.5. Engineered nanomaterial exposure

1 mL of 20 nm naïve Au-ENM spheres was prepared by sonicating the ENM in stock solution for 2 min. A single bolus dose of 0.9 mL stock solution (5775.94 ng/mL) was administered and infused into the proximal uterine artery through a 3-way stopcock. Distal maternal and

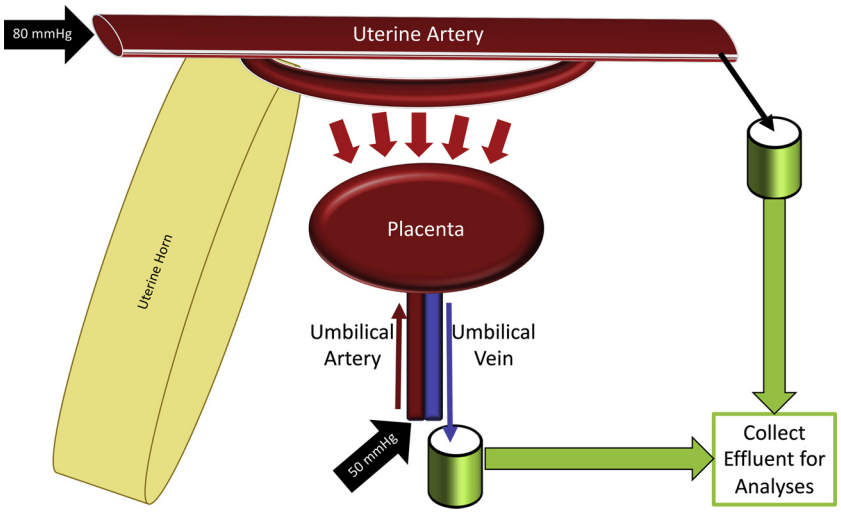

Fig. 1. Schematic of placental perfusion methodology. Isolation of the uterine horn and placental unit permits cannulation of the proximal uterine artery and umbilical vein; perfusion of these arteries allows for perfusion and countercurrent flow within the placenta. Cannulation of the distal uterine artery and umbilical artery allow for effluent collection for biochemical and physiological analyses.

fetal umbilical effluents were collected every 10 min for 180 min for analysis.

2.6. Histology and pathology assessments

After perfusion, placentas were fixed in a 10% neutral buffered formalin prior to processing and paraffin embedding. Haemotoxylin and eosin (H&E) stained sections were assessed by an ACVP board-certified veterinary pathologist.

2.7. Material visualization

Histological placental sections were visualized *via* transmitted darkfield hyperspectral images and data captured using CytoViva darkfield optics at 60× magnification with oil objective. Hyperspectral imaging provides a spectral analysis permitting differentiation between particles. Dual Mode Fluorescence (DMF) images were captured with Texas Red excitation filter and triple pass emission filter to allow for visualization of fluorescent and non-fluorescent particles simultaneously. Data was processed using ENVI 4.8 (CytoViva, Auburn, AL).

2.8. Sample preparation for ICP-MS analysis

Au-ENM perfusion effluent was prepared by dissolving ~50–200 µL of sample in aqua regia (3:1, [HCl]:[HNO_3]). No difference was found between ambient temperature digestion and microwave digestion for the Au-ENM in physiological salt solution (PSS). Therefore, all subsequent samples were digested at ambient temperature in acid-cleaned polypropylene centrifuge tubes. Control samples (*i.e.* PSS spiked with Au-ENM) were digested alongside the perfused samples to monitor Au recovery and matrix effects.

Tissue samples (~0.2 g) were weighed into 50 mL polypropylene centrifuge tubes and homogenized by ultra-sonicating in 1 mL of concentrated HNO_3. The samples were allowed to react and degas overnight and subsequently digested using a CEM MARS X microwave digestion system, applying the following procedure (Table 1).

Control samples (*i.e.* tissue not treated with Au-ENM perfusion) were digested alongside the perfused samples and spiked with Au to monitor recovery and matrix effects. All digested samples were diluted to 3% HCl:1% HNO_3 in preparation for analysis by inductively coupled plasma mass spectrometry (ICP-MS).

2.9. Measurement with ICP-MS

Au concentrations were measured at mass 197 on a Nu AttoM high resolution ICP-MS, at low resolution (300). The operating conditions were as follows: RF power of 1550 W, carrier gas flow of 1.00 L/min Ar, and nebulizer gas flow of ~36 psi Ar. Three replicates of ^{197}Au were measured in deflector jump mode with 20 µs peak dwell time, 500 sweeps, and 10 cycles.

Table 1
Tissue digestion parameters for detection of Au-ENM using CEM MARS X.

Step	Power		Time (min)
1	300 W	75%	5
2	300 W	100%	5
3	300 W	100%	5
4	300 W	100%	5
5	300 W	100%	10
6	300 W	100%	10
7	300 W	100%	10
8	300 W	100%	10

Standards were prepared daily with Au concentrations ranging from 0.001 to 5 ppb, in 3% HCl:1% HNO_3. Sample concentrations were determined using a linear regression through at least five standards, with a correlation coefficient > 0.999 for all runs. Matrix matched quality control standards were repeatedly measured after every sixth sample to account for instrument drift and monitor reproducibility. Quality control standards reproduced with RSD $< 5\%$ ($n = 2–7$ depending on number of samples in the batch).

To reduce Au memory effect, a washout solution containing 3% HCl:1% HNO_3 + 0.2% L-cysteine was used following each sample for 3 min to mobilize remnant Au, then followed with clean 3% HCl:1% HNO_3. Au memory effect was further monitored by bracketing samples with clean acid carryover (3% HCl:1% HNO_3) following the washout, and detection limit was reduced to 0.001 ppb for effluent analyses and 0.005 ppb for tissue analyses.

2.10. Fluid flow across the placenta

After equilibration, effluent was collected at 10-min intervals from the maternal and fetal segments for 180 min. This fluid was weighed to quantify the rate of fluid that passage through the uterine artery or placenta and umbilical vein and identify any decreases in fluid flow within the system attributed to ENM infusion.

2.11. Statistics

Au-ENM transport at baseline and through the maternal and fetal effluents was analyzed by each time point compared to control measurements with Student's *T*-test. Significance was set at $p < 0.05$ and a

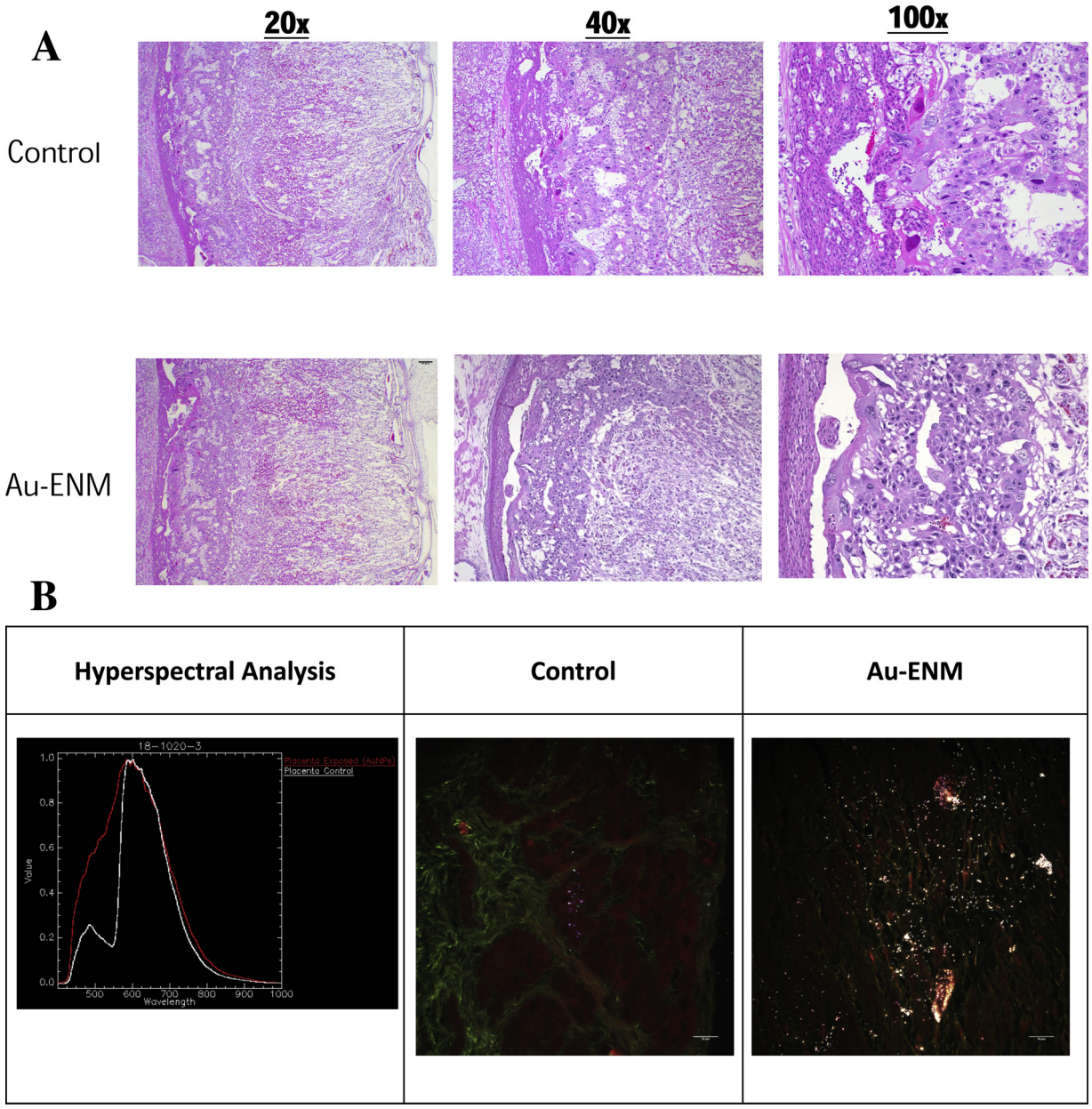

Fig. 2. Representative images of placental morphology after *ex vivo* perfusion. (A) There was no identifiable histopathology associated with Au-ENM exposure or perfusion pressures in any of the samples (n = 3). (B) Identification and visualization of Au-ENM particle deposition within the placenta after material infusion and placental perfusion using enhanced hyperspectral microscopy (CytoViva, Inc). While xenobiotic particles were identified in the control samples, these particles exhibit a different hyperspectral waveform compared to the Au-ENM samples.

trend (T) was identified as $p < 0.1$. SEM is reported.

3. Results

Initial verification of the model was necessary to confirm that all histological and morphological membranes remain intact during *ex vivo* perfusion of the placenta. Samples were reviewed by a veterinary pathologist and no pathological damage was identified (Fig. 2a), indicating that translocation within the system is due to normal physiological function of the placenta. Fig. 2b identifies the passage of Au-ENM through hyperspectral analysis and darkfield microscopy. The hyperspectral analysis provides a spectral response associated with Au-ENM exposure (red) compared to control (white) and image of the reflectance of the Au-ENM deposition within the placental tissue.

Au-ENM transfer to maternal vasculature was confirmed with significant translocation across the uterine artery within 20 min after Au-ENM infusion (Fig. 3a). This significance remains for all 180 min after bolus material infusion. Further, significant concentrations of Au-ENM were detected in the fetal compartment within 20 min of uterine artery infusion (Fig. 3b). These results confirmed Au-ENM passage from maternal-fetal tissues to the fetal compartment.

This model was used not only to calculate the amount of material passaging through the system, but to document the physiological response within the *ex vivo* system. In this respect, there was no significant decrease in maternal artery fluid flow after Au-ENM infusion (Fig. 4a).

However, there were significant reductions in fluid flow across the placenta and to the umbilical vein and fetal compartment after Au-ENM uterine infusion (Fig. 4b). While calculated significance varied in the time post-material infusion, any reduction in blood flow to the developing fetal pup could have serious consequences to fetal growth, nutrient delivery, and waste exchange.

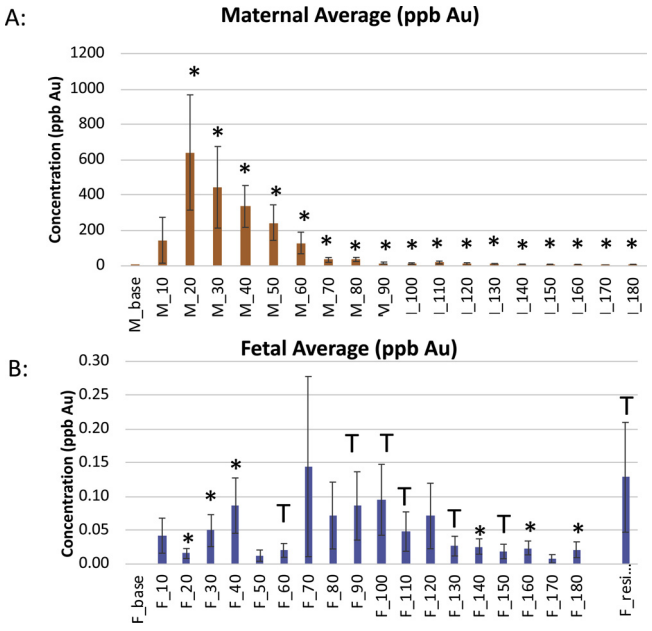

Fig. 3. Quantification of Au-ENM concentration within the (A) uterine artery effluents and (B) fetal umbilical vein effluents over a 180-min time course *via* ICP-MS analyses, normalized and compared to baseline. *$p < 0.05$; $^{T}p < 0.1$. (n = 11).

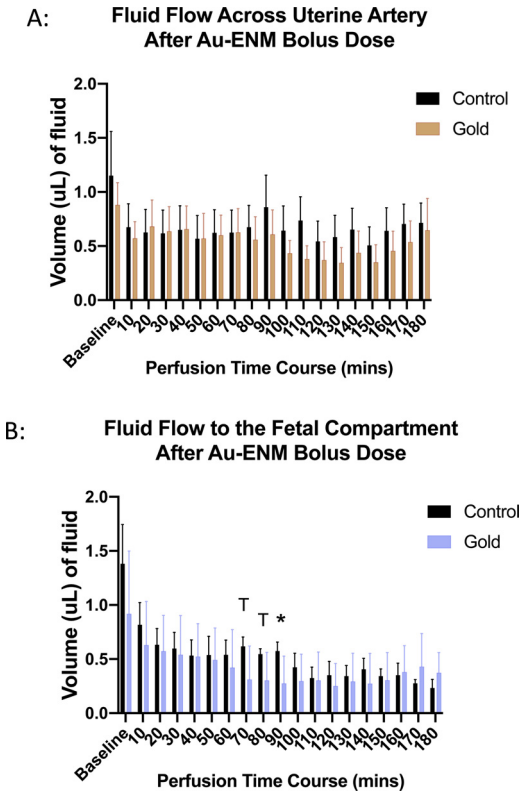

Fig. 4. Measurement of (A) maternal fluid flow across the uterine artery or (B) fluid flow across the placenta to the fetal compartment after Au-ENM infusion. *$p < 0.05$; $^{T}p < 0.1$. compared to control values. (n = 11).

Finally, we quantified total Au-ENM transfer during the placental perfusion within the maternal effluents, uterine muscle and vasculature, placenta and fetal umbilical effluent. From the total Au-ENM that was recovered, there was an average of 77.8% found in the maternal effluent, 17.4% within the uterine muscle and vasculature, 6.17% placenta and 0.065% within the fetal effluent (Fig. 5).

4. Discussion

Using novel techniques and methodology, these studies identified a time course of *ex vivo* material transfer and quantified a reduction of fluid flow across the placenta after ENM infusion into the maternal uterine artery. Through the development and implementation of this novel *ex vivo* placental perfusion technique we were able to quantify Au-ENM 3 h after material infusion. In preparation for ICP-MS analyses, improvements to tissue preparation and material extraction methodologies were also developed. To our knowledge, this is the first application of rodent placental perfusion to directly assess the physiological implication to fluid transport and placental barrier function after naïve Au-ENM exposure.

The changes to fluid flow quantified within this system lend validity to measurements previously made within our laboratory identifying hemodynamic abnormalities in uterine basal arterioles 24-h after a single inhalation exposure to nanosized titanium dioxide (TiO_2) aerosols using intravital microscopy to visualize the intact uterine vasculature [39]. After chronic inhalation exposure to TiO_2 ENM aerosols we identified endothelium-dependent dysfunction in isolated radial arterioles compared to control [40]. Maternal ENM exposures during pregnancy have significant implications to fetal development and fetal health [12]. These include reduced maternal weight gain, fetal number, fetal weight, neonatal weight [40,41], and increased reabsorption sites [42]. Furthermore, uterine and umbilical vascular dysfunction is evident after both chronic and acute maternal exposure to ENM during pregnancy, limiting resources to developing fetal pups downstream [39,40,42,43]. Fetal exposure during gestation culminates in reduced fetal health including impaired neonatal growth, epigenetic modifications, coronary and vascular dysfunction, metabolic complications, pulmonary impairments, and neurodevelopmental changes [40,44–50]. These effects may be attributed to maternal inflammation [39], neurological impacts [51], maternal physiological adaptations associated with exposure [40,41,52], and/or direct engineered nanomaterial translocation to the fetus [53–55].

While the results associated with material and fluid transfer to the fetal compartment include some trending differences, we would contend that the identification of any xenobiotic material within the fetal compartment and any reduction of blood flow would have physiological implications to uterine health and could have long lasting effects on fetal development. If offspring were to survive, this exposure may be a platform for the developmental onset of future adult disease. While not all post-infusion time points reached statistical significance, even subtle hemodynamic changes may be detrimental to fetal growth. Taken together, these studies indicate a reduction in blood flow from the uterine circulation to the fetal compartment after maternal ENM exposure. This reduction in blood puts the developing fetus at risk of ischemia, hypoxia, hyponutrition, intrauterine growth restriction, and death.

One drawback of the *ex vivo* rat placental perfusion is a partial loss of the original dose administered in two ways. Because we did not cannulate the maternal uterine vein, this remains an opening for loss of dose through the maternal venous system. There is also additional loss to be accounted for within the plastic tubing and glass pipette cannulas, as Au may stick to these surfaces while passing through the system. Future work should include maternal uterine vein cannulation to capture test article that is sent back through venous circulation.

Other groups have initiated *ex vivo* rodent perfusion studies to evaluate microvascular function of the placenta after dam ENM inhalation [56]. These studies have focused on uterine vascular reactivity post-exposure, providing further evidence of uteroplacental dysfunction after maternal ENM exposure. The distinctions of our methodology involve the umbilical vasculature cannulations, cross-perfusion of the placenta, and toxicological assessment of the fetal compartment. One

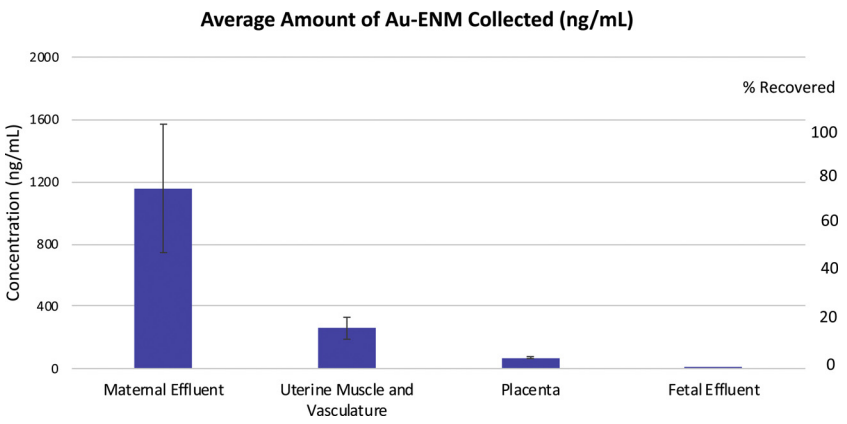

Fig. 5. Total Au-ENM transfer after the perfusion experiment was complete *via* ICP-MS analyses. These represent the distribution of Au-ENM within the maternal effluents (time course samples pooled), uterine muscle and vasculature, placenta and fetal effluents (time course samples pooled). Data is represented as quantified deposition (left) and percentage of material collected (right).

study to date evaluates maternal-fetal transfer after chronic nose-only ENM exposure [53]; however, it is unclear if this is a cumulative outcome or if ENM transfer to and deposition within the fetus may occur after a single exposure.

Human placental perfusion studies are performed using a single cotyledon, due to variability of deposition within the tissue, the physiological function of the entire organ should be considered. Further, human tissue has logistical considerations with respect to access and previous exposure(s) during gestation [19–22]. The improvement of analytical techniques in the last decade may account for differences between laboratories. For example, the study examining PEG-Au-ENM using human cotyledon perfusion by Myllynen (2008) found no material transfer; whereas PEG-Au-ENM was identified by Aengenheister (2018) using similar methodology. As these techniques continue to advance, measurements of the transfer of material associated with real-world dosages will become readily available.

In vitro toxicological studies of placental transport focus on the use of immortal trophoblasts (BeWo cells) and are limited to the confines of a cell culture model including the use of immortal cell lines, high treatment dosages, and lack a physiological system (tissue support, fluid flows) [20,24,57,58]. On the other hand, *in vivo* studies have traditionally used high doses of a single intravenously injected ENM to track movement and material deposition [13,15–18]. Fortunately, more sensitive analytical techniques have become available to help identify and quantify these materials.

Overall, these studies highlight the rapid transport of Au-ENM from the maternal uterine vasculature to the fetal compartment. These data are vital for future development of biomedical products using Au-ENM as a vehicle or functionalized backbone. These studies provide a platform for the development of perinatal therapies targeted for fetal treatment and a methodology to assess the likelihood of fetal avoidance during drug development. Manipulation of the Au-ENM physiochemical properties and addition of functionalized groups will allow for the design of targeted therapies for placental interaction or for avoidance of cellular uptake within the uteroplacental system [8,9]. In addition, using an *ex vivo* rodent model with many pups per pregnancy would allow for multiple studies to be completed with a single animal. Future studies using this *ex vivo* methodology will not only identify xenobiotic transfer, but also include biochemical assessments of the maternal and fetal effluents to quantify changes to placental function, identify markers and gender-specific adaptations of placental stress, decreases in oxygen tension, and vasoactive metabolites to assess perinatal health.

Acknowledgements

This work was supported by the National Institute of Environmental Health Sciences (R00-ES024783), Rutgers Center for Environmental Exposures and Disease (P30-ES005022), and Rutgers Joint Graduate Program in Toxicology (T32-ES007148). Thank you to Adam Goodwill for assistance in designing Fig. 1. Thank you to CytoViva, Inc for their assistance with Fig. 2B.

References

[1] P.G. Thorpe, S.M. Gilboa, S. Hernandez-Diaz, J. Lind, J.D. Cragan, G. Briggs, S. Kweder, J.M. Friedman, A.A. Mitchell, M.A. Honein, National Birth Defects Prevention Study, Medications in the first trimester of pregnancy: most common exposures and critical gaps in understanding fetal risk, Pharmacoepidemiol. Drug Saf. 22 (9) (2013) 1013–1018.
[2] S.A. Rasmussen, Human teratogens update 2011: can we ensure safety during pregnancy? Birth Defects Res. Part A: Clin. Mol. Teratol. 94 (3) (2012) 123–128.
[3] D. Cabuzu, A. Cirja, R. Puiu, A.M. Grumezescu, Biomedical applications of gold nanoparticles, Curr. Top. Med. Chem. 15 (16) (2015) 1605–1613.
[4] N. Elahi, M. Kamali, M.H. Baghersad, Recent biomedical applications of gold nanoparticles: a review, Talanta 184 (2018) 537–556.
[5] N. Khlebtsov, V. Bogatyrev, L. Dykman, B. Khlebtsov, S. Staroverov, A. Shirokov, L. Matora, V. Khanadeev, T. Pylaev, N. Tsyganova, G. Terentyuk, Analytical and theranostic applications of gold nanoparticles and multifunctional nanocomposites, Theranostics 3 (3) (2013) 167–180.
[6] M.M. Mahan, A.L. Doiron, Gold nanoparticles as X-ray, CT, and multimodal imaging contrast agents: formulation, targeting, and methodology, J. Nanomater. 2018 (2018) 15.
[7] R. Cheheltani, R.M. Ezzibdeh, P. Chhour, K. Pulaparthi, J. Kim, M. Jurcova, J.C. Hsu, C. Blundell, H.I. Litt, V.A. Ferrari, H.R. Allcock, C.M. Sehgal, D.P. Cormode, Tunable, biodegradable gold nanoparticles as contrast agents for computed tomography and photoacoustic imaging, Biomaterials 102 (2016) 87–97.
[8] S.B. Fournier, J.N. D'Errico, P.A. Stapleton, Engineered nanomaterial applications in perinatal therapeutics, Pharmacol. Res. 130 (2018) 36–43.
[9] J.N. D'Errico, P.A. Stapleton, Developmental onset of cardiovascular disease - could the proof be in the placenta? Microcirculation (2018) e12526.
[10] P.A. Stapleton, Gestational nanomaterial exposures: microvascular implications during pregnancy, fetal development and adulthood, J. Physiol. 594 (8) (2016) 2161–2173.
[11] P.A. Stapleton, T.R. Nurkiewicz, Maternal nanomaterial exposure: a double threat to maternal uterine health and fetal development? Nanomedicine (Lond.) 9 (7) (2014) 929–931.
[12] K.S. Hougaard, L. Campagnolo, P. Chavatte-Palmer, A. Tarrade, D. Rousseau-Ralliard, S. Valentino, M.V. Park, W.H. de Jong, G. Wolterink, A.H. Piersma, B.L. Ross, G.R. Hutchison, J.S. Hansen, U. Vogel, P. Jackson, R. Slama, A. Pietroiusti, F.R. Cassee, A perspective on the developmental toxicity of inhaled nanoparticles, Reprod. Toxicol. 56 (2015) 118–140.
[13] S. Sweeney, A. Adamcakova-Dodd, P.S. Thorne, J.G. Assouline, Multifunctional nanoparticles for real-time evaluation of toxicity during fetal development, PLoS One 13 (2) (2018) e0192474.
[14] X.F. Zhang, J.H. Park, Y.J. Choi, M.H. Kang, S. Gurunathan, J.H. Kim, Silver nanoparticles cause complications in pregnant mice, Int. J. Nanomed. 10 (2015) 7057–7071.
[15] L. Campagnolo, M. Massimiani, G. Palmieri, R. Bernardini, C. Sacchetti, A. Bergamaschi, L. Vecchione, A. Magrini, M. Bottini, A. Pietroiusti, Biodistribution and toxicity of pegylated single wall carbon nanotubes in pregnant mice, Part. Fibre Toxicol. 10 (2013) 21.
[16] R.W. Snyder, T.R. Fennell, C.J. Wingard, N.P. Mortensen, N.A. Holland, J.H. Shannahan, W. Pathmasiri, A.H. Lewin, S.C. Sumner, Distribution and biomarker of carbon-14 labeled fullerene C60 ([(14) C(U)]C60) in pregnant and lactating rats and their offspring after maternal intravenous exposure, J. Appl. Toxicol. 35 (12) (2015) 1438–1451.
[17] M. Semmler-Behnke, J. Lipka, A. Wenk, S. Hirn, M. Schaffler, F. Tian, G. Schmid, G. Oberdorster, W.G. Kreyling, Size dependent translocation and fetal accumulation of gold nanoparticles from maternal blood in the rat, Part. Fibre Toxicol. 11 (2014) 33.
[18] K. Yamashita, Y. Yoshioka, K. Higashisaka, K. Mimura, Y. Morishita, M. Nozaki, T. Yoshida, T. Ogura, H. Nabeshi, K. Nagano, Y. Abe, H. Kamada, Y. Monobe,

T. Imazawa, H. Aoshima, K. Shishido, Y. Kawai, T. Mayumi, S. Tsunoda, N. Itoh, T. Yoshikawa, I. Yanagihara, S. Saito, Y. Tsutsumi, Silica and titanium dioxide nanoparticles cause pregnancy complications in mice, Nat. Nanotechnol. 6 (5) (2011) 321–328.

[19] L. Aengenheister, D. Dietrich, A. Sadeghpour, P. Manser, L. Diener, A. Wichser, U. Karst, P. Wick, T. Buerki-Thurnherr, Gold nanoparticle distribution in advanced in vitro and ex vivo human placental barrier models, J. Nanobiotechnol. 16 (1) (2018) 79.

[20] P.K. Myllynen, M.J. Loughran, C.V. Howard, R. Sormunen, A.A. Walsh, K.H. Vahakangas, Kinetics of gold nanoparticles in the human placenta, Reprod. Toxicol. 26 (2) (2008) 130–137.

[21] P. Wick, A. Malek, P. Manser, D. Meili, X. Maeder-Althaus, L. Diener, P.A. Diener, A. Zisch, H.F. Krug, U. von Mandach, Barrier capacity of human placenta for nanosized materials, Environ. Health Perspect. 118 (3) (2010) 432–436.

[22] S. Grafmueller, P. Manser, L. Diener, P.A. Diener, X. Maeder-Althaus, L. Maurizi, W. Jochum, H.F. Krug, T. Buerki-Thurnherr, U. von Mandach, P. Wick, Bidirectional transfer study of polystyrene nanoparticles across the placental barrier in an ex vivo human placental perfusion model, Environ. Health Perspect. 123 (12) (2015) 1280–1286.

[23] S. Grafmueller, P. Manser, L. Diener, L. Maurizi, P.A. Diener, H. Hofmann, W. Jochum, H.F. Krug, T. Buerki-Thurnherr, U. von Mandach, P. Wick, Transfer studies of polystyrene nanoparticles in the ex vivo human placenta perfusion model: key sources of artifacts, Sci. Technol. Adv. Mater. 16 (4) (2015) 044602.

[24] L. Aengenheister, K. Keevend, C. Muoth, R. Schonenberger, L. Diener, P. Wick, T. Buerki-Thurnherr, An advanced human in vitro co-culture model for translocation studies across the placental barrier, Sci. Rep. 8 (1) (2018) 5388.

[25] B.V. Sastry, Techniques to study human placental transport, Adv. Drug Deliv. Rev. 38 (1) (1999) 17–39.

[26] N. Goeden, A. Bonnin, Ex vivo perfusion of mid-to-late-gestation mouse placenta for maternal-fetal interaction studies during pregnancy, Nat. Protoc. 8 (1) (2013) 66–74.

[27] N. Goeden, F.M. Notarangelo, A. Pocivavsek, S. Beggiato, A. Bonnin, R. Schwarcz, Prenatal dynamics of kynurenine pathway metabolism in mice: focus on kynurenic acid, Dev. Neurosci. 39 (6) (2017) 519–528.

[28] C.S. Rosenfeld, Sex-specific placental responses in fetal development, Endocrinology 156 (10) (2015) 3422–3434.

[29] M.J. Soares, K. Iqbal, K. Kozai, Hypoxia and placental development, Birth Defects Res. 109 (17) (2017) 1309–1329.

[30] J.N. D'Errico, S.B. Fournier, P.A. Stapleton, *Ex vivo* perfusion of the rodent placenta, J. Vis. Exp. 147 (2019) e59412.

[31] H. Bond, B. Baker, R.D. Boyd, E. Cowley, J.D. Glazier, C.J. Jones, C.P. Sibley, B.S. Ward, S.M. Husain, Artificial perfusion of the fetal circulation of the in situ mouse placenta: methodology and validation, Placenta 27 (Suppl. A) (2006) S69–75.

[32] T. Nishimura, T. Chishu, M. Tomi, R. Nakamura, K. Sato, N. Kose, Y. Sai, E. Nakashima, Mechanism of nucleoside uptake in rat placenta and induction of placental CNT2 in experimental diabetes, Drug Metab. Pharmacokinet. 27 (4) (2012) 439–446.

[33] J. Stulc, B. Stulcova, S. Husain, C.P. Sibley, Transfer of Cl- across placenta of anesthetized rat, Am. J. Physiol. 271 (5 Pt. 2) (1996) R1107–14.

[34] J. Stulc, B. Stulcova, Placental transfer of phosphate in anaesthetized rats, Placenta 17 (7) (1996) 487–493.

[35] J. Stulc, B. Stulcova, J. Svihovec, Transport of calcium across the dually perfused placenta of the rat, J. Physiol. 420 (1990) 295–311.

[36] P. Pavek, Z. Fendrich, F. Staud, J. Malakova, H. Brozmanova, M. Laznicek, V. Semecky, M. Grundmann, V. Palicka, Influence of P-glycoprotein on the transplacental passage of cyclosporine, J. Pharm. Sci. 90 (10) (2001) 1583–1592.

[37] P. Pavek, F. Staud, Z. Fendrich, H. Sklenarova, A. Libra, M. Novotna, M. Kopecky, M. Nobilis, V. Semecky, Examination of the functional activity of P-glycoprotein in the rat placental barrier using rhodamine 123, J. Pharmacol. Exp. Ther. 305 (3) (2003) 1239–1250.

[38] P. Kafka, O. Vajnerova, J. Herget, V. Hampl, Rho-kinase inhibition attenuates acute hypoxic fetoplacental vasoconstriction in the rat, Physiol. Res. 61 (Suppl. 2) (2012) S43–8.

[39] P.A. Stapleton, C.R. McBride, J. Yi, A.B. Abukabda, T.R. Nurkiewicz, Estrous cycle-dependent modulation of in vivo microvascular dysfunction after nanomaterial inhalation, Reprod. Toxicol. 78 (2018) 20–28.

[40] P.A. Stapleton, V.C. Minarchick, J. Yi, K. Engels, C.R. McBride, T.R. Nurkiewicz, Maternal engineered nanomaterial exposure and fetal microvascular function: does the Barker hypothesis apply? American Journal of Obstetrics and Gynecology 209 (3) (2013) e1–11 227.

[41] K.S. Hougaard, P. Jackson, Z.O. Kyjovska, R.K. Birkedal, P.J. De Temmerman, A. Brunelli, E. Verleysen, A.M. Madsen, A.T. Saber, G. Pojana, J. Mast, A. Marcomini, K.A. Jensen, H. Wallin, J. Szarek, A. Mortensen, U. Vogel, Effects of lung exposure to carbon nanotubes on female fertility and pregnancy. A study in mice, Reprod. Toxicol. 41 (2013) 86–97.

[42] S.B. Fournier, S. Kallontzi, L. Fabris, C. Love, P.A. Stapleton, Effect of gestational age on maternofetal vascular function following single maternal engineered nanoparticle exposure, Cardiovasc. Toxicol. (2019).

[43] A.K. Vidanapathirana, L.C. Thompson, E.E. Mann, J.T. Odom, N.A. Holland, S.J. Sumner, L. Han, A.H. Lewin, T.R. Fennell, J.M. Brown, C.J. Wingard, PVP formulated fullerene (C60) increases Rho-kinase dependent vascular tissue contractility in pregnant Sprague Dawley rats, Reprod. Toxicol. 49 (2014) 86–100.

[44] J.L. Blum, J.Q. Xiong, C. Hoffman, J.T. Zelikoff, Cadmium associated with inhaled cadmium oxide nanoparticles impacts fetal and neonatal development and growth, Toxicol. Sci. (2012).

[45] J.L. Blum, J.Q. Xiong, C. Hoffman, J.T. Zelikoff, Cadmium associated with inhaled cadmium oxide nanoparticles impacts fetal and neonatal development and growth, Toxicological Sciences : An Official Journal of the Society of Toxicology 126 (2) (2012) 478–486.

[46] Q.A. Hathaway, C.E. Nichols, D.L. Shepherd, P.A. Stapleton, S.L. McLaughlin, J.C. Stricker, S.L. Rellick, M.V. Pinti, A.B. Abukabda, C.R. McBride, J. Yi, S.M. Stine, T.R. Nurkiewicz, J.M. Hollander, Maternal-engineered nanomaterial exposure disrupts progeny cardiac function and bioenergetics, Am. J. Physiol. Heart Circ. Physiol. 312 (3) (2017) H446–H458.

[47] E. Paul, M.L. Franco-Montoya, E. Paineau, B. Angeletti, S. Vibhushan, A. Ridoux, A. Tiendrebeogo, M. Salome, B. Hesse, D. Vantelon, J. Rose, F. Canoui-Poitrine, J. Boczkowski, S. Lanone, C. Delacourt, J.C. Pairon, Pulmonary exposure to metallic nanomaterials during pregnancy irreversibly impairs lung development of the offspring, Nanotoxicology 11 (4) (2017) 484–495.

[48] M. Umezawa, A. Onoda, I. Korshunova, A.C.O. Jensen, I.K. Koponen, K.A. Jensen, K. Khodosevich, U. Vogel, K.S. Hougaard, Maternal inhalation of carbon black nanoparticles induces neurodevelopmental changes in mouse offspring, Part. Fibre Toxicol. 15 (1) (2018) 36.

[49] E.B. Engler-Chiurazzi, P.A. Stapleton, J.J. Stalnaker, X. Ren, H. Hu, T.R. Nurkiewicz, C.R. McBride, J. Yi, K. Engels, J.W. Simpkins, Impacts of prenatal nanomaterial exposure on male adult Sprague-Dawley rat behavior and cognition, J. Toxicol. Environ. Health A 79 (11) (2016) 447–452.

[50] T. Notter, L. Aengenheister, U. Weber-Stadlbauer, H. Naegeli, P. Wick, U. Meyer, T. Buerki-Thurnherr, Prenatal exposure to TiO2 nanoparticles in mice causes behavioral deficits with relevance to autism spectrum disorder and beyond, Transl. Psychiatry 8 (1) (2018) 193.

[51] P.A. Stapleton, A.B. Abukabda, S.L. Hardy, T.R. Nurkiewicz, Xenobiotic pulmonary exposure and systemic cardiovascular response via neurological links, Am. J. Physiol. Heart Circ. Physiol. 309 (10) (2015) H1609–H1620.

[52] K.S. Hougaard, P. Jackson, K.A. Jensen, J.J. Sloth, K. Loschner, E.H. Larsen, R.K. Birkedal, A. Vibenholt, A.M. Boisen, H. Wallin, U. Vogel, Effects of prenatal exposure to surface-coated nanosized titanium dioxide (UV-titan). A study in mice, Part. Fibre Toxicol. 7 (2010) 16.

[53] L. Campagnolo, M. Massimiani, L. Vecchione, D. Piccirilli, N. Toschi, A. Magrini, E. Bonanno, M. Scimeca, L. Castagnozzi, G. Buonanno, L. Stabile, F. Cubadda, F. Aureli, P.H. Fokkens, W.G. Kreyling, F.R. Cassee, A. Pietroiusti, Silver nanoparticles inhaled during pregnancy reach and affect the placenta and the foetus, Nanotoxicology 11 (5) (2017) 687–698.

[54] C.A. Austin, G.K. Hinkley, A.R. Mishra, Q. Zhang, T.H. Umbreit, M.W. Betz, E. Wildt B, B.J. Casey, S. Francke-Carroll, S.M. Hussain, S.M. Roberts, K.M. Brown, P.L. Goering, Distribution and accumulation of 10 nm silver nanoparticles in maternal tissues and visceral yolk sac of pregnant mice, and a potential effect on embryo growth, Nanotoxicology 10 (6) (2016) 654–661.

[55] C.A. Austin, T.H. Umbreit, K.M. Brown, D.S. Barber, B.J. Dair, S. Francke-Carroll, A. Feswick, M.A. Saint-Louis, H. Hikawa, K.N. Siebein, P.L. Goering, Distribution of silver nanoparticles in pregnant mice and developing embryos, Nanotoxicology 6 (2012) 912–922.

[56] A.B. Abukabda, E.C. Bowdridge, C.R. McBride, T.P. Batchelor, W.T. Goldsmith, K.L. Garner, S. Friend, T.R. Nurkiewicz, Maternal titanium dioxide nanomaterial inhalation exposure compromises placental hemodynamics, Toxicol. Appl. Pharmacol. 367 (2019) 51–61.

[57] H. Tang, Z. Jiang, H. He, X. Li, H. Hu, N. Zhang, Y. Dai, Z. Zhou, Uptake and transport of pullulan acetate nanoparticles in the BeWo b30 placental barrier cell model, Int. J. Nanomed. 13 (2018) 4073–4082.

[58] E.K. Muller, C. Grafe, F. Wiekhorst, C. Bergemann, A. Weidner, S. Dutz, J.H. Clement, Magnetic nanoparticles interact and pass an in vitro co-culture blood-placenta barrier model, Nanomaterials (Basel) 8 (2) (2018).